

Supporting Information for: Radiolabeling and In Vivo Evaluation of Lanmodulin with Biomedically Relevant Lanthanide Isotopes

Table of Contents

Experimental Procedures	2
1. General Methods	2
2. Production of LanM	4
3. Synthesis of Tagged Constructs, LanM-PSMA and DFO-LanM	5
3.1 Synthesis of PSMA-mal	5
3.2 Conjugation of PSMA to LanM	8
3.3 Conjugation of DFO to LanM	10
4. Preliminary Radiolabeling of LanM and Optimization of Radiolabeling Yield .12	
5. Radiolabeling and Characterization of wt LanM	12
6. Radiolabeling of Tagged Constructs, LanM-PSMA and DFO-LanM	16
7. Mammalian Cell Binding Determination	17
8. Ex Vivo Biodistribution and Metabolite Analysis	18
8.1 ¹⁷⁷Lu Conjugate Naïve Biodistribution	18
8.2 ^{132/135}La Conjugate Naïve Biodistribution	20
8.3 ^{132/135}La Conjugate Targeted Biodistribution	22
8.4 ⁸⁹Zr Conjugate Naïve Biodistribution	24
9. PET Imaging	24
10. References	25

Experimental Procedures

1. General Methods

All chemicals were obtained from commercial suppliers in biochemical reagent grade or better and used without further purification. *E. coli* BL21(DE3) cells were obtained from New England Biolabs (NEB). NMR spectra (^1H , ^{13}C) were collected on a 700 MHz Advance III Bruker instrument at 25 °C and processed using TopSpin 4.0.7. Chemical shifts are reported as parts per million (ppm). Mass spectrometry of protein constructs was performed at the Proteomics and Mass Spectrometry Core Facility at Penn State. The mass spectra were acquired on a Bruker Ultraflex extreme MALDI TOF-TOF instrument using a factory-configured instrument method for the linear positive-ion detection over the 5,000 – 20,000 m/z range. Laser power attenuation and pulsed ion extraction time were optimized to achieve the best signal. The instrument was calibrated with a five-protein mixture containing bovine insulin (MW 5,733.6), bovine ubiquitin (MW 8,564.8), horse heart cytochrome C (MW 12,360.1), bovine ribonuclease A (MW 13,682.3), and horse heart apomyoglobin (MW 16,951.5). Mass spectra were smoothed (Savitzky-Golay, width 5 m/z , 1 cycle) and baseline subtracted (TopHat). Mass lists were generated using a centroid peak detection algorithm. High-resolution electrospray ionization (ESI) mass spectrometry of small molecules was carried out at the Stony Brook University Center for Advanced Study of Drug Action (CASDA) with a Bruker Impact II UHR QTOF MS system. Gel filtration chromatography was performed on an automated GE Healthcare Biosciences Akta Pure fast protein liquid chromatography system (FPLC). Preparative high performance liquid chromatography (HPLC) was carried out on a Phenomenex Luna C18 column (250 mm \times 21.2 mm, 100 Å, AXIA packed) at a flow rate of 15 mL/min using

a Shimadzu HPLC-20AR equipped with a binary gradient pump, UV-vis detector, and manual injector. UV absorption was recorded at 254 nm. Method A (Solvent A=H₂O+0.1% TFA (trifluoroacetic acid) and B=MeCN+0.1% TFA): Gradient: 0–1 min: 5% B; 1–14 min: 5–50% B; 14–23 min: 50–95% B; 23–26 min: 95% B; 26–27 min: 95–5% B; 27–30 min: 5% B. Analytical HPLC was carried out on a Phenomenex Luna 5 μm C18 column (150 mm × 3 mm, 100 Å, AXIA packed) at a flow rate of 0.8 mL/min using a Shimadzu HPLC-20AR equipped with a binary gradient pump, UV-vis detector, autoinjector, and Laura radiodetector. Method B (Solvent A=H₂O+0.1% TFA and B=MeCN+0.1% TFA): Gradient: 0–2 min: 5% B; 2–14 min: 5–95% B; 14–16 min: 95% B; 16–16.5 min: 95–5% B; 16.5–20 min 5% B. RadioHPLC analysis was carried out on the Shimadzu HPLC-20AR equipped with a binary gradient, pump, UV-Vis detector, autoinjector and a Laura radiodetector on a Phenomenex Yarra-2000 size exclusion column using an isocratic gradient (Method C: 3 μm, 145 Å, 150 × 7.8 mm; Solvent: 30 mM MOPS (3-(N-morpholino)propanesulfonic acid), 100 mM KCl, pH = 7.0; 0.75 mL/min). Inductively couple plasma-optical emission spectrometry (ICP-OES) was carried out using an Agilent 5110 ICP-OES. A 6-point standard curve with a check standard with respect to lutetium and lanthanum was used and fits were found to be at least R² of 0.9999. Concentrations were then back calculated to the sample stock concentration. Positron emission tomography (PET) imaging was conducted using Siemens Inveon PET/CT Multimodality System and data reconstruction was done using ASIPro software and AMIDE. ¹⁷⁷LuCl₃ was obtained from the Department of Energy (DOE) isotope program, produced at the University of Missouri reactor. ^{132/135}LaCl₃ and ⁸⁹Zr-oxalate were obtained from the Engle Lab at University of Wisconsin-Madison.

All animal experiments were conducted according to the guidelines of the Institutional Animal Care and Use Committee (IACUC) at Stony Brook Medicine.

2. Production of LanM

Wild type (WT) LanM was produced as described.³ Cys-LanM (WT LanM with a Gly-Ser-Gly-Cys peptide added to the C-terminus) was purified as described.² Briefly, plasmids containing genes encoding for each protein were obtained from TWIST Bioscience (pET-29b(+)-LanM). The proteins were grown in chemically competent *E. coli* BL21(DE3) cells (NEB), which were grown at 37 °C in lysogeny broth (LB). Isopropyl β -d-1-thiogalactopyranoside (IPTG, 200 μ M) was added at $OD_{600nm} = \sim 0.6$ to induce overexpression for 3 h at 37 °C. Cells were lysed by sonication and loaded to a gravity-flow 25-mL (2.5 \times 5 cm) Q-Sepharose Fast Flow column and eluted using a 80 \times 80 mL, 0.01 – 1 M NaCl gradient. Dithiothreitol (DTT, 10 mM) was included in these buffers for Cys-LanM purification to minimize thiol oxidation. LanM-containing fractions were identified by SDS-PAGE analysis and then purified using gel filtration chromatography (HiLoad 16/600 Superdex 75 pg). For Cys-LanM purifications, 5 mM DTT was included. LanM- or Cys-LanM-containing fractions were collected and concentrated to ~ 2.0 mM. LanM was stored in 30 mM MOPS, 100 mM KCl, 5% glycerol, pH 7.0 and Cys-LanM was stored in the same buffer containing 5 mM DTT.

¹H NMR (700 MHz, CD₃OD): δ 7.77 (m, 3H, H^{21,24,26}), 7.67 (s, 1H, H¹⁹), 7.42 (m, 2H, H^{22,27}), 7.38 (d, 1H, H²³), 6.77 (s, 2H, H^{43, 44}), 4.67 (t, 1H, H¹⁶), 4.32 (q, 1H, H²), 4.19 (q, 1H, H⁹), 3.47 (t, 2H, H⁴¹), 3.24 (m, 1H, H¹⁷), 3.12 (t, 2H, H¹⁴), 3.07 (m, 1H, H¹⁷), 2.98 (d, 2H, H³⁵), 2.40 (m, 2H, H⁴), 2.16 (m, 4H, H^{3, 29, 37}), 1.89 (m, 1H, H³), 1.78 (m, 2H, H^{30, 31}), 1.68 (m, 2H, H^{33, 11}), 1.59 (m, 6H, H^{11, 38, 30, 32}), 1.36 (m, 4H, H^{30, 34, 13}), 1.27 (m, 5H, H^{32, 12, 39}), 0.92 (m, 2H, H^{31, 33}). **¹³C{¹H} NMR** (175 MHz, CD₃OD): δ 178.9 (C⁵), 176.4 (C^{1,10}), 176.0 (C³⁶), 176.0 (C²⁸), 173.7 (C¹⁵), 172.6 (C^{42,45}), 160.1 (C⁷), 135.9 (C¹⁸), 135.3 (C^{43,44}), 134.9 (C²⁵), 133.9 (C²⁰), 129.0 (C^{21,24}), 128.6 (C²⁷), 128.5 (C^{19,26}), 127.1 (C²²), 126.6 (C²³), 55.9 (C¹⁶), 53.9 (C⁹), 53.5 (C²), 46.4 (C³⁵), 45.9 (C²⁹), 39.3 (C¹⁴), 39.3 (C¹⁷), 38.5 (C⁴¹), 38.4 (C³⁷), 36.8 (C³⁴), 32.8 (C¹¹), 31.1 (C⁴), 31.0 (C⁴⁰), 30.9 (C³⁹), 30.3 (C³¹), 29.8 (C³³), 29.6 (C¹³), 29.3 (C³⁸), 28.9 (C³), 27.3 (C³²), 26.6 (C³⁰), 23.6 (C¹²).

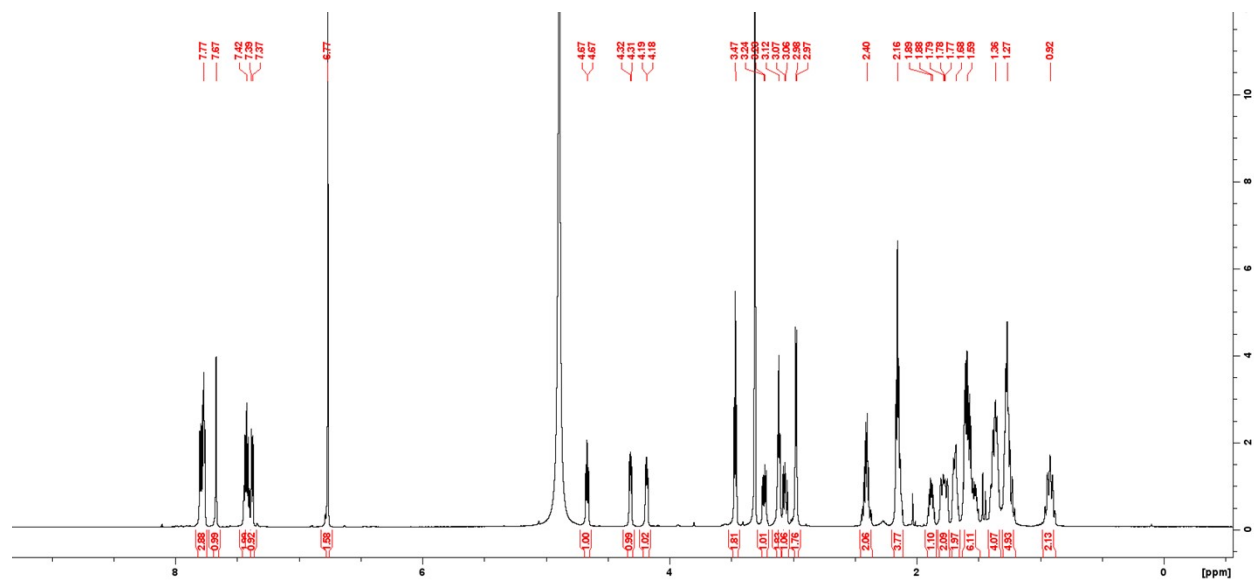


Figure S1. ¹H NMR of PSMA-mal. 700 MHz, CD₃OD.

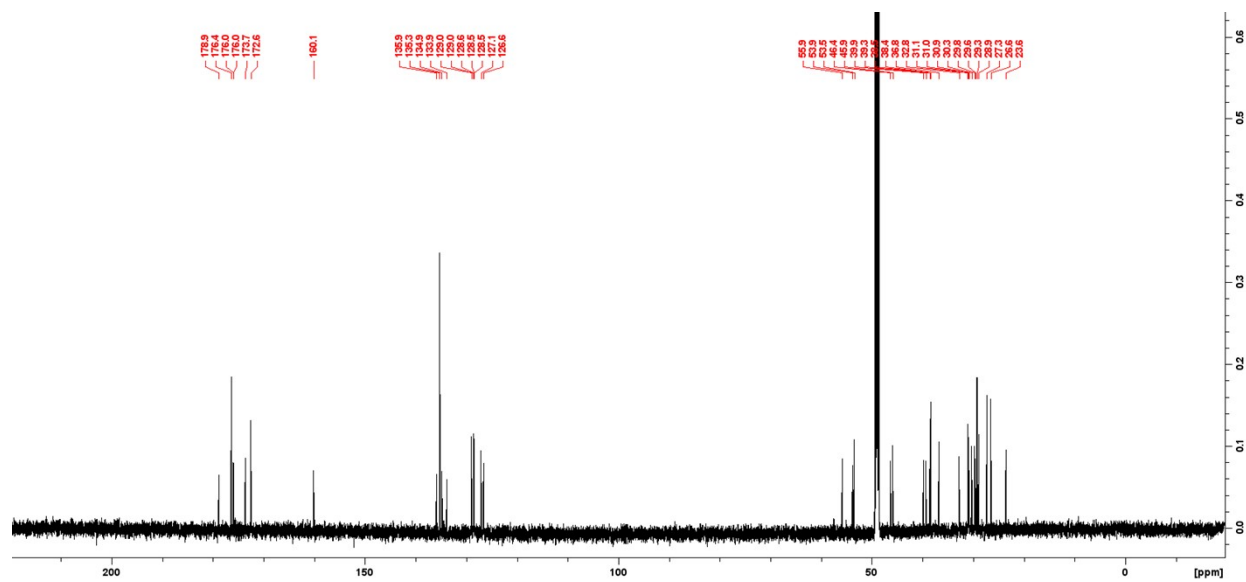


Figure S2. $^{13}\text{C}\{^1\text{H}\}$ NMR of PSMA-mal. 175 MHz, CD_3OD .

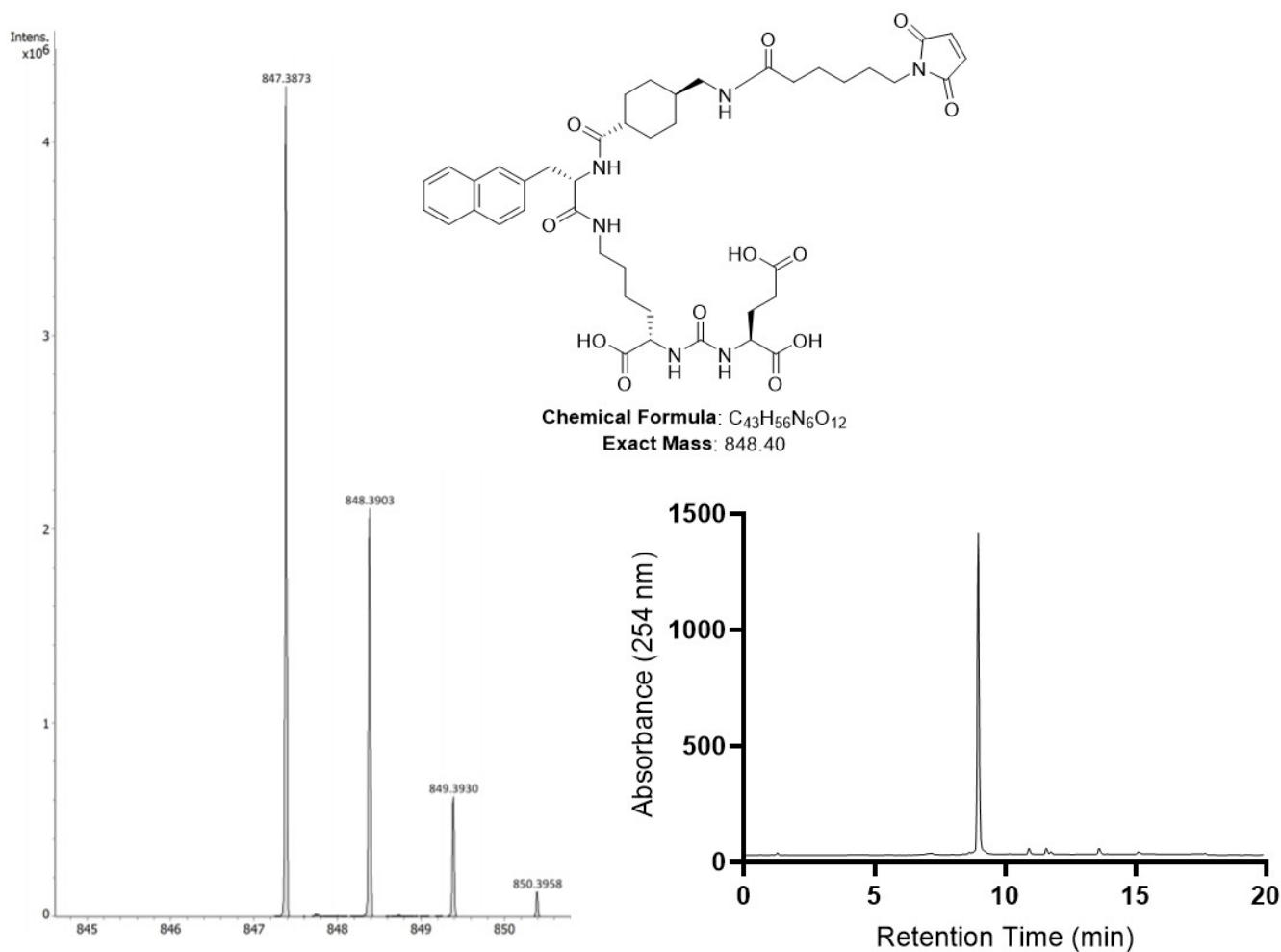


Figure S3. Characterization data [HRMS, left, and analytical HPLC ($t_R = 9.0$ min, Method B), right] of PSMA-mal.

3.2 Conjugation of PSMA to LanM

PSMA-mal was dissolved in pure dimethyl sulfoxide (DMSO, ~25 mg/mL or 25 mM). In a 1.7 mL tube, 222 μ L Cys-LanM (1.8 mM) and 650 μ L buffer (50 mM Tris (trisaminomethane), 100 mM KCl, 10 mM TCEP (tris(2-carboxyethyl) phosphine), pH 7.4) were mixed and incubated for 2 min. Then, 128 μ L of PSMA-mal (25 mM) were added dropwise over 1 min while mixing to prevent precipitation. The reaction mixture was nutated at 4 $^{\circ}$ C overnight. The resulting mixture was centrifuged at 12000 $\times g$ for 2 min to

remove precipitate. The reaction product was confirmed in the remaining aqueous phase

by mass spectrometry and subsequently purified using analytical-scale gel filtration chromatography (HiLoad 10/300 Superdex 75 pg, 1 mL loop, 0.75 mL/min) using 30 mM MOPS, 100 mM KCl, 5% glycerol, pH 7.0 (no reductant). The protein conjugate eluted from the column over the course of 2 mL.

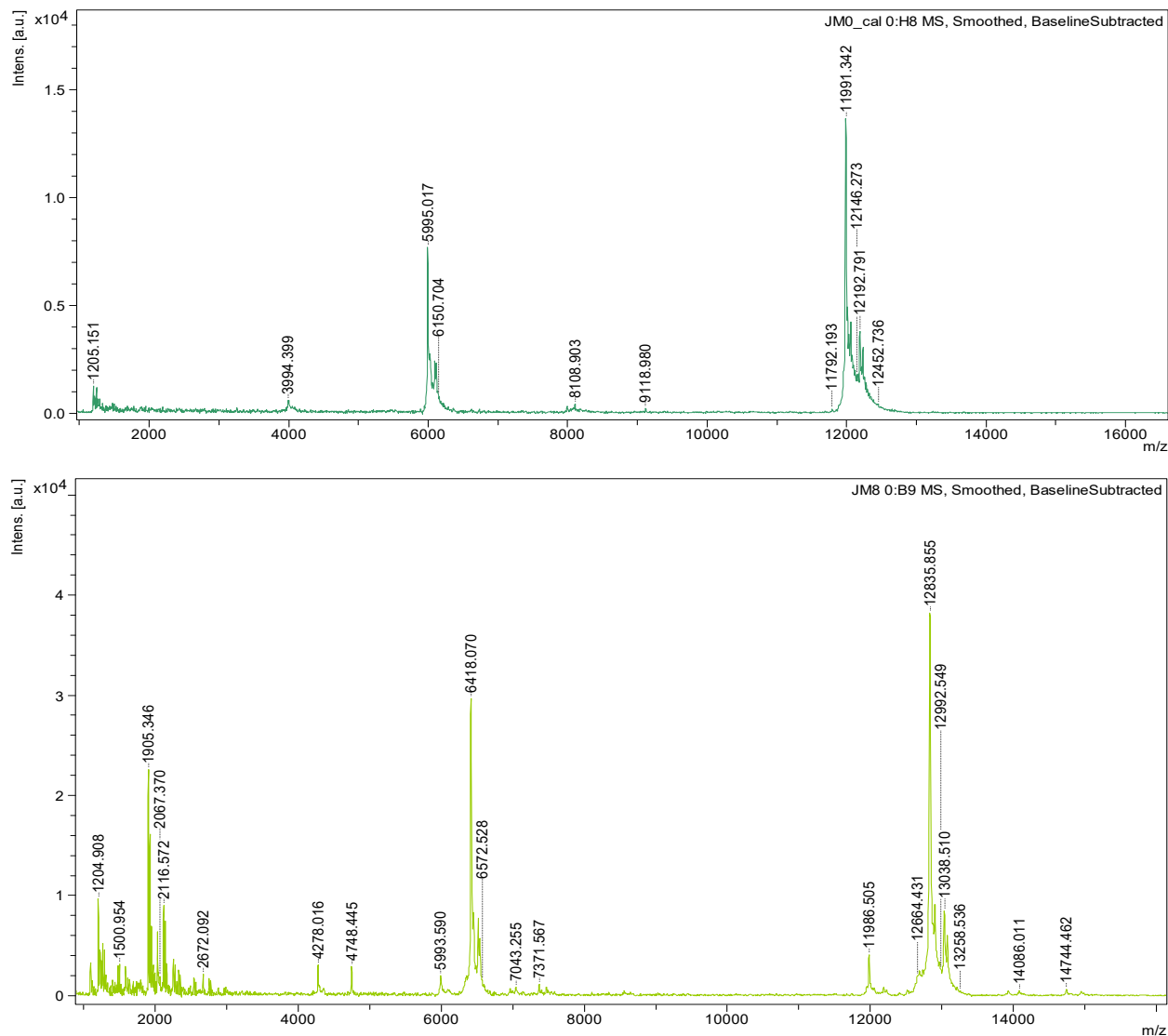


Figure S4. Mass spectrometry analysis of Cys-LanM starting material (top) and raw reaction product (bottom). Samples were exchanged into pure H₂O to a final concentration of 20-80 μ M using 7-kDa MWCO Zeba spin filtration devices. (Top) The primary peak at $m/z = 11991$ Da and secondary peak at $m/z = 5995$ Da correspond to Cys-LanM ($z = 1$ and $z = 2$, respectively). (Bottom) The primary peak at $m/z = 12836$ Da and secondary peak at $m/z = 6418$ Da both correspond to PSMA-labeled LanM ($z = 1$ and $z = 2$, respectively).

3.3 Conjugation of DFO to LanM

p-SCN-Bn-desferrioxamine (DFO-NCS) (752.9 g/mol) was obtained from Macrocyclics, Inc. and dissolved in pure DMSO (~20 mg/mL or 25 mM). In a 15 mL conical tube, 5.4 mL of 100 mM KCl, 500 μ L LanM (2.0 mM stock concentration), and 8.0 μ L LaCl₃ (250 mM stock concentration) were combined to produce La₂LanM. To this mixture, 4.0 mL of 100 mM NaHCO₃, 100 mM KCl, pH 9.0 was added. This order of addition is important to prevent precipitation of lanthanum carbonate. Finally, 10 \times 10 μ L additions of DFO-NCS (25 mM or 5 mg/264 μ L) were added, with thorough mixing between each addition. Final reaction mixture was 100 μ M La₂LanM and 250 μ M DFO-NCS, which was nutated overnight at room temperature. Product was spun down (12,000 $\times g$ for 2 min) to remove precipitate and concentrated to ~400 μ L using an Amicon Ultra 10-kDa molecular weight cut off (MWCO) centrifugal filter device. >50% incorporation of DFO-NCS was confirmed by mass spectrometry through formation of peaks at m/z values integer multiples of 752 above LanM base mass of 11686 Da (Figure S5).

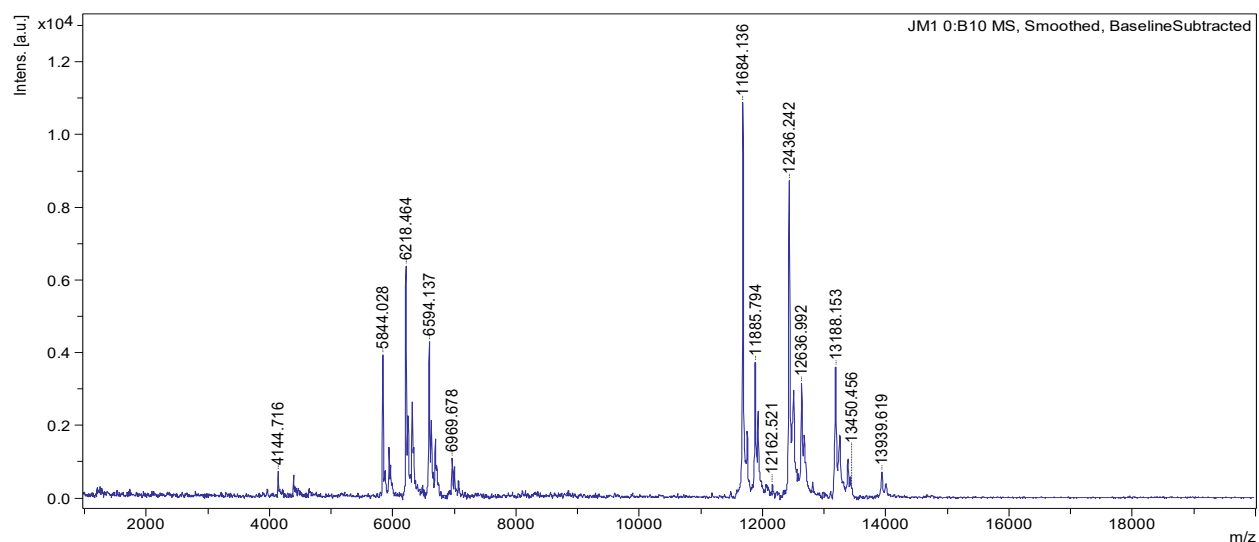
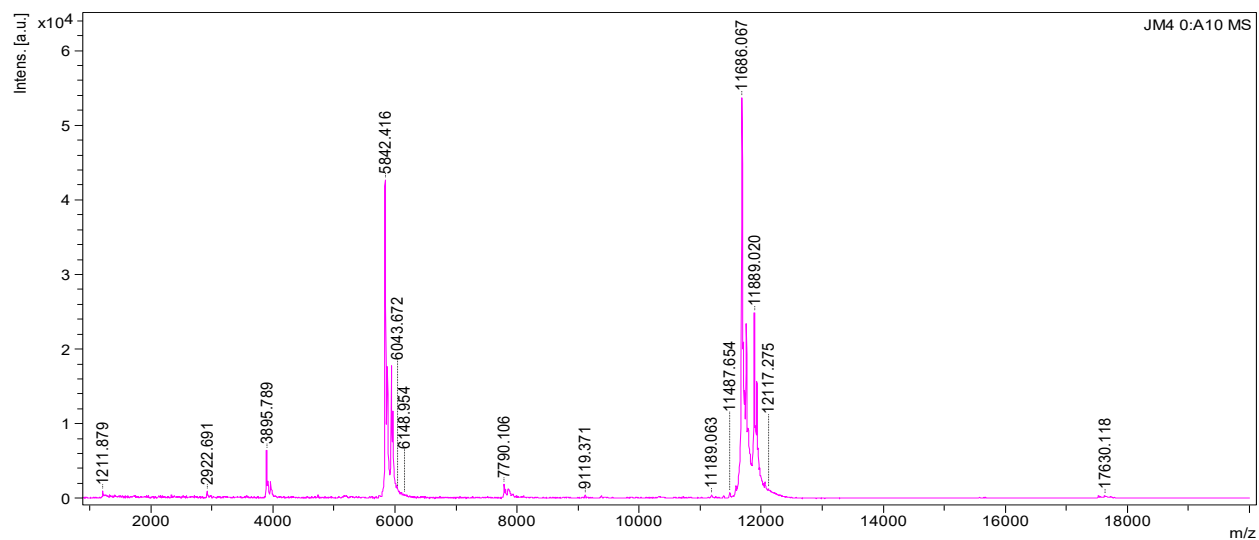


Figure S5. Mass spectrometry analysis of LanM starting material (top) and raw reaction product (bottom). Samples were exchanged into pure H₂O to a final concentration of 20-80 μ M using 7-kDa MWCO Zeba spin filtration devices. (Top) The primary peak at $m/z = 11686$ Da and secondary peak at $m/z = 5842$ Da correspond to LanM ($z = 1$ and $z = 2$ respectively). (Bottom) The primary high molecular weight peaks at $m/z = 11684$, 12436, and 13188 Da and secondary peaks at $m/z = 5844$, 6218, and 6594 Da correspond to the $z = 1$ and $z = 2$ peaks of LanM(DFO)_n, with $n = 0, 1$, and 2.

Spectrofluorometric Titration of LanM with Citrate

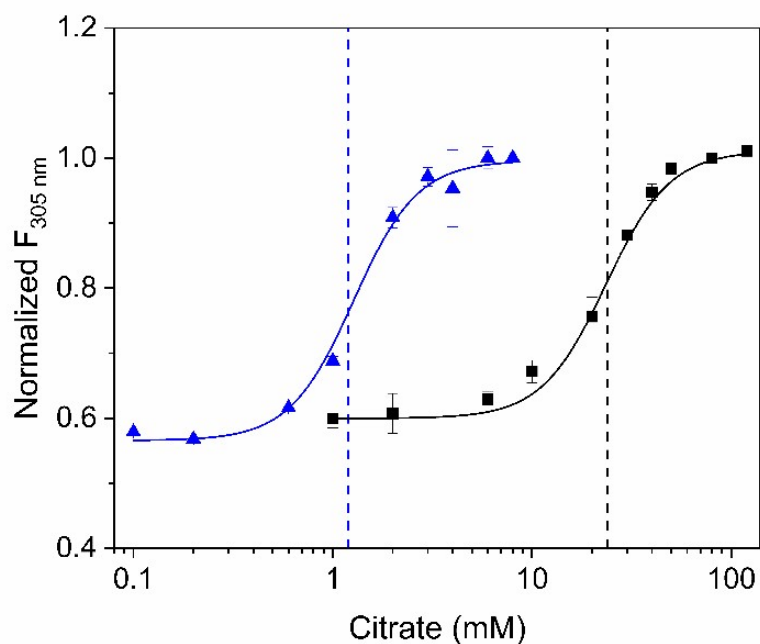


Figure S6. Spectrofluorometric titration of LanM, bound to 2 equiv. La(III) (black) or Lu(III) (blue) with citrate. The titration is followed using the fluorescence emission of Tyr96, the sole tyrosine in the protein, the fluorescence emission intensity of which decreases in the presence of lanthanide(III) ions^{1,2} (and increases when those ions are desorbed from protein by citrate). $[\text{Citrate}]_{1/2}$ values are annotated as dashed lines; 1.2 ± 0.1 mM for Lu(III) and 24 ± 2 mM for La(III), respectively. Excitation at 278 nm, emission at 305 nm. Buffer: 20 mM acetate, 100 mM KCl, pH 5.0.

4. Preliminary Radiolabeling of LanM and Optimization of Radiolabeling Yield

Caution! Work with radioactive isotopes such as ^{177}Lu , $^{132/135}\text{La}$, and ^{89}Zr should only be carried out by trained personnel at facilities approved and equipped to safely handle these isotopes.

To assess the ideal amount of non-radioactive metal to be added to maximize radiolabeling yields, LanM (20 nmol in 30 mM MOPS 100 mM KCl pH 7.0 buffer) was incubated with $^{177}\text{LuCl}_3$ (3.6 MBq-3.9 MBq/98-105 μCi) and various equivalents of $^{\text{nat}}\text{LuCl}_3$ (1-4 equiv. relative to protein concentration, 5.0 mM) for 30 min. Samples were injected on the radioHPLC and extent of radiolabeling was determined by integration of the resulting radioactive peak.

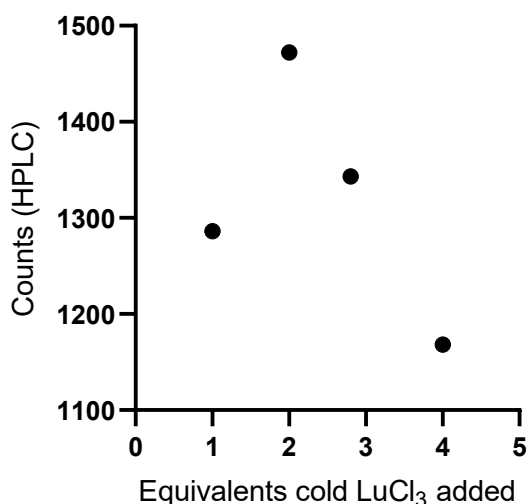


Figure S7. Optimization of radiolabeling conditions

5. Radiolabeling and Characterization of wt LanM

Lu-177 labeling. Radiolabeling with ^{177}Lu was performed by mixing 37 MBq (1.0 mCi ^{177}Lu for ^{177}Lu -Lu-LanM) or 126 MBq (3.40 mCi ^{177}Lu for ^{177}Lu -La-LanM) with 20 nmol of protein

in 30 mM MOPS, 100 mM KCl, pH 7.0. Subsequently, 2 equivalents of non-radioactive metal ($^{nat}\text{LuCl}_3$, 8 μL , 5.0 mM or $^{nat}\text{LaCl}_3$, 10.3 μL , 3.88 mM) were added. Samples was allowed to react for 90 min at room temperature and then purified using Zeba spin desalting columns (7k MWCO). A radiochemical yield of 75.4% for $^{177}\text{Lu-Lu-LanM}$ and 20.6% for $^{177}\text{Lu-La-LanM}$ were achieved.

La-132/135 labeling. Radiolabeling with $^{132/135}\text{La}$ was performed by mixing 11 MBq (0.3 mCi $^{132/135}\text{La}$) of radiometal with 20 nmol of protein in 30 mM MOPS, 100 mM KCl, 5% glycerol, pH 7.0. Subsequently, 2 equivalents of non-radioactive metal ($^{nat}\text{LaCl}_3$, 7.6 μL , 5.22 mM) were added. Samples were allowed to react for 90 min at room temperature and then purified using Zeba spin desalting columns (7k MWCO). A radiochemical yield of 28.4% was achieved.

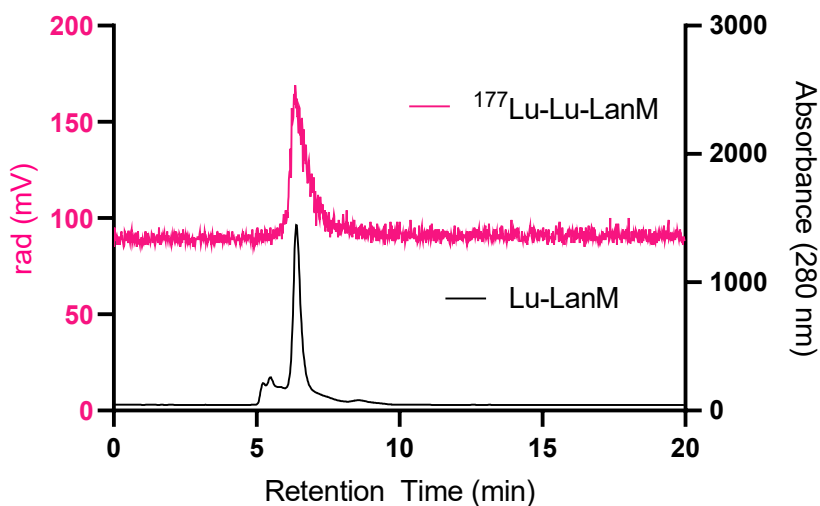


Figure S8. Radiolabeling of $^{177}\text{Lu-Lu-LanM}$ ($t_R = 6.4$ min, Method C) overlaid with LanM complexed with 3 eq of ^{nat}Lu ($t_R = 6.4$ min, Method C).

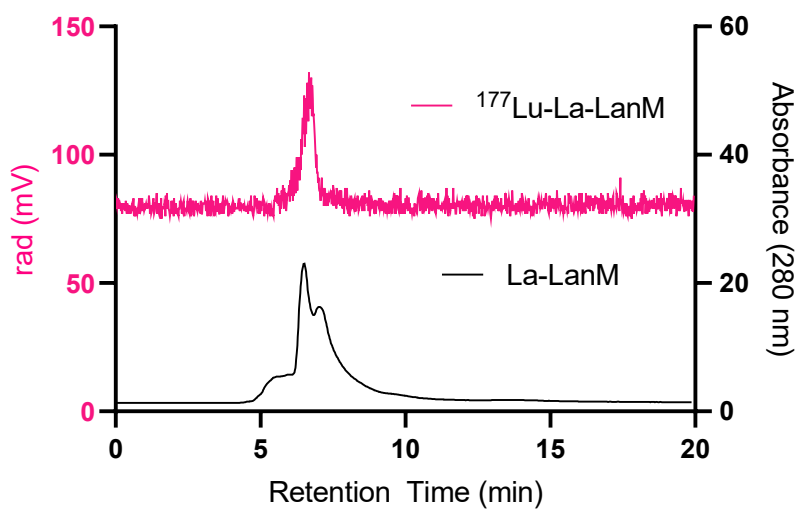


Figure S9. Radiolabeling of ^{177}Lu -La-LanM ($t_R = 6.6$ min, Method C) overlaid with LanM complexed with 2 eq of $^{\text{nat}}\text{La}$ ($t_R = 6.5$ min, Method C).

Radiolabeling with $^{132/135}\text{La}$ was performed by mixing 11 MBq (0.3 mCi $^{132/135}\text{La}$) of radiometal with 20 nmol of protein in 30 mM MOPS 100 mM KCl, 5% glycerol pH 7.0 buffer solution. Subsequently, 2 equivalents of non-radioactive metal ($^{\text{nat}}\text{LaCl}_3$, 7.6 μL , 5.22 mM) were added. Samples were allowed to react for 90 minutes at room temperature and then purified using Zeba Spin Desalting Columns (7k MWCO). A radiochemical yield after purification of 28.4% was achieved.

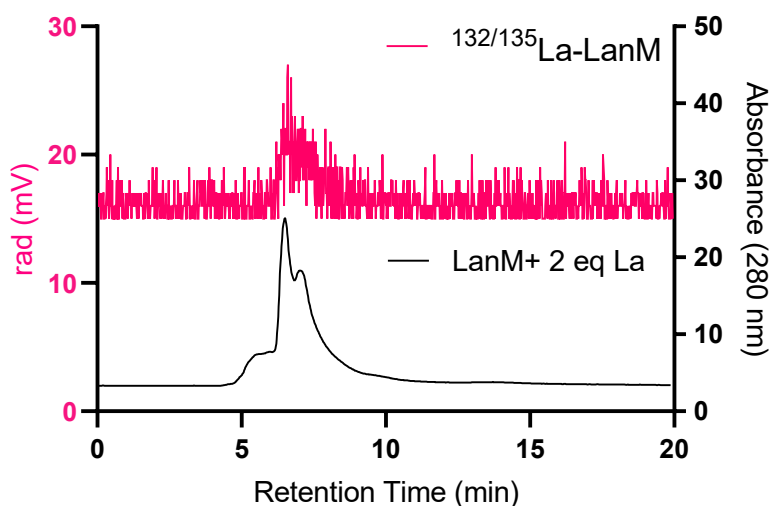


Figure S10. Radiolabeling of $^{132/135}\text{La-LanM}$ ($t_R = 6.6$ min, Method C) overlaid with LanM complexed with 2 eq of $^{\text{nat}}\text{La}$ ($t_R = 6.5$ min, Method C).

6. Radiolabeling of Tagged Constructs, LanM-PSMA and DFO-LanM

Radiolabeling of LanM-PSMA with $^{132/135}\text{La}$ was performed by mixing 35 MBq (940 μCi $^{132/135}\text{La}$) of radiometal with 20 nmol of protein in 30 mM MOPS, 100 mM KCl, pH 7.0. Subsequently, 2 equivalents of non-radioactive metal ($^{\text{nat}}\text{LaCl}_3$, 8.6 μL , 4.66 mM) were added. Samples were allowed to react for 90 minutes at room temperature and then purified using Zeba Spin Desalting Columns (7k MWCO). A radiochemical yield after purification of 16.4% was achieved.

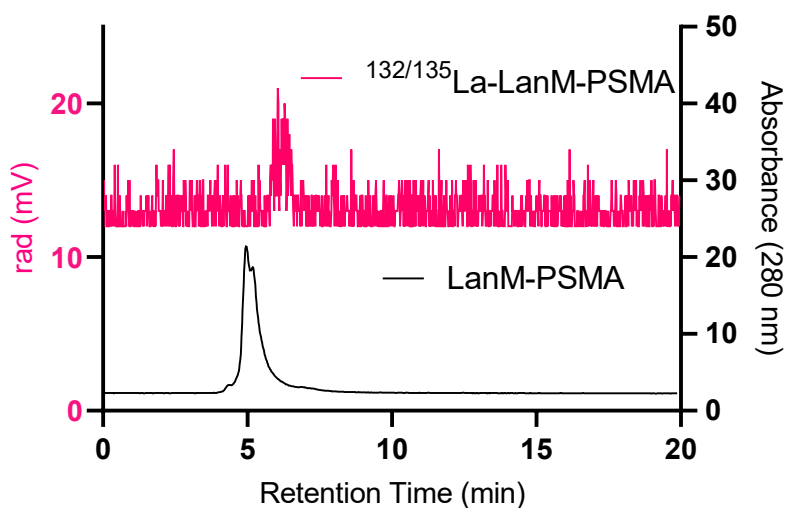


Figure S11. Radiolabeling of $^{132/135}\text{La-LanM-PSMA}$ ($t_R = 6.1$ min, Method C) overlaid with LanM-PSMA ($t_R = 5.2$ min, Method C).

^{89}Zr -oxalate was pH-adjusted using 0.1 M Na_2CO_3 to pH 7.0. Radiolabeling with ^{89}Zr was then performed by mixing 35.7 MBq (965 μCi ^{89}Zr) of radiometal with 20 nmol of DFO-LanM in 30 mM MOPS, 100 mM KCl, pH 7.0. Samples were allowed to react for 90 min at room temperature and then purified using Zeba spin desalting columns (7k MWCO). A radiochemical yield of 82.5% yield was achieved.

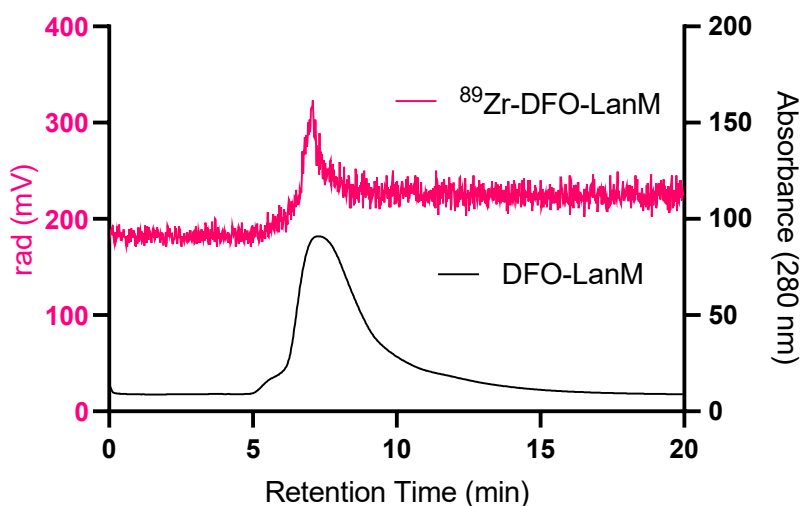


Figure S12. Radiolabeling of ^{89}Zr -DFO-LanM ($t_R = 7.1$ min, Method C) overlaid with DFO-LanM ($t_R = 7.3$ min, Method C).

7. Mammalian Cell Binding Determination

Cells were maintained in standard supplemented media (DMEM, 10% FBS, 1% penicillin/streptomycin) at 37 °C and 5% CO_2 . PC3 PiP or PC3 Flu cells were seeded in 24-well plates ($\sim 5 \times 10^5$ cells in 2 mL standard growth medium/well) allowing adhesion and growth overnight. The cells were washed twice with PBS prior to the addition of cell culture medium (965 μL /well) and $^{132/135}\text{La}$ -LanM-PSMA (2.6 μCi per well, 35 μL diluted in phosphate buffered saline). The well-plates were incubated for 2 h at 37 °C and 5% CO_2 . To determine the uptake of radioligand, cells were washed three times with ice-cold PBS and then lysed by addition of NaOH (1 M, 1.5 mL) to each well. The radioactivity was quantified by gamma counting and expressed as percent activity relative to initial added activity. Cell binding data were assessed by unpaired t-tests using GraphPad Prism to determine if differences between groups were statistically significant ($p < 0.05$).

8. Ex Vivo Biodistribution and Metabolite Analysis

All animal experiments were approved by and conducted according to the guidelines of the Institutional Animal Care and Use Committee (IACUC) at Stony Brook Medicine.

8.1 ^{177}Lu Conjugate Naïve Biodistribution

Male mice (BALB/c) were injected with ^{177}Lu -Lu-LanM (2.5-2.8 MBq/68-77 μCi), ^{177}Lu -La-LanM (2.1-2.8 MBq/56-75 μCi) or $^{177}\text{LuCl}_3$ (0.5-1.3 MBq/17-36 μCi). After 2 h, animals were sacrificed by cervical dislocation and selected tissues were collected and weighed. Activity of tissues was counted using a γ -counter (1470 PerkinElmer Wizard) and the radioactivity associated with each organ was expressed as % ID/g. To assess the presence of intact LanM protein remaining, urine was directly injected to the radioHPLC and the resulting trace was compared to that of the radiolabeled protein.

Table S1. Biodistribution of ^{177}Lu -Lu-LanM, ^{177}Lu -La-LanM, $^{177}\text{LuCl}_3$

Organ	^{177}Lu -Lu-LanM 2h (n=3)	^{177}Lu -La-LanM 2h (n=4)	$^{177}\text{LuCl}_3$ 2h (n=3)
Blood	3.26 \pm 0.41	3.06 \pm 0.83	6.01 \pm 1.81
Heart	3.02 \pm 1.68	1.64 \pm 0.23	3.11 \pm 0.92
Lung	3.43 \pm 0.09	2.92 \pm 0.47	4.84 \pm 0.95
Liver	4.59 \pm 0.12	3.39 \pm 0.28	19.27 \pm 0.69
Spleen	1.75 \pm 0.18	1.26 \pm 0.26	6.40 \pm 1.22
Kidney	14.30 \pm 2.57	9.22 \pm 1.90	5.72 \pm 0.94
Sm Int	3.09 \pm 1.19	2.12 \pm 0.48	2.63 \pm 1.27
Muscle	1.26 \pm 0.25	0.84 \pm 0.09	0.95 \pm 0.21
Bone	8.89 \pm 3.15	11.10 \pm 2.57	8.30 \pm 4.47

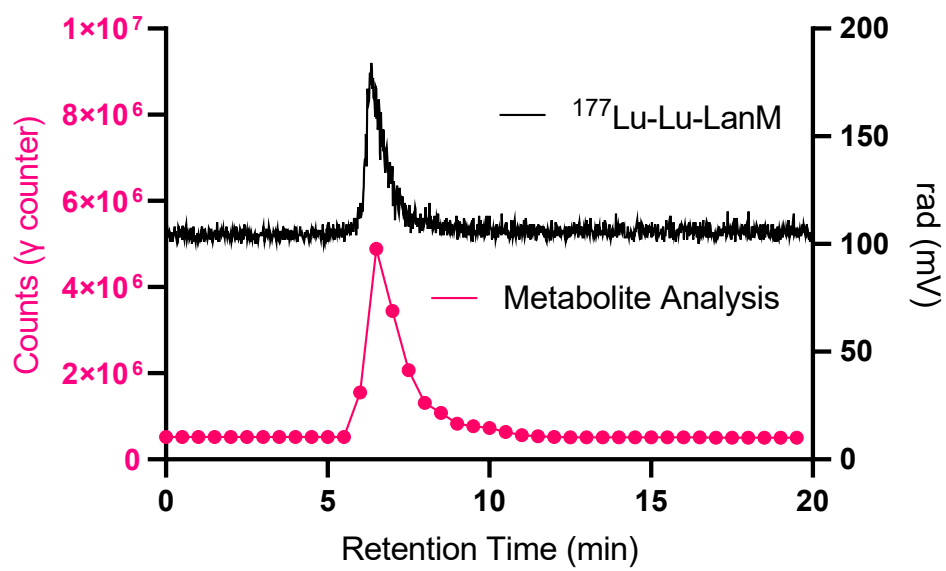


Figure S13. Metabolite analysis of $^{177}\text{Lu-Lu-LanM}$ compared to radiolabeling trace.

8.2 ^{132/135}La Conjugate Naïve Biodistribution

Male mice (14 weeks old, Jackson Laboratories, C57BL/6J) were injected with ^{132/135}La-LanM (0.37 MBq-0.52 MBq/10-14 µCi) or ^{132/135}La-citrate (0.33-0.52 MBq/ 9-14 µCi). After 2 h, animals were sacrificed by cervical dislocation and selected tissues were collected and weighed. Activity of tissues was counted using a γ-counter (1470 PerkinElmer Wizard), and the radioactivity associated with each organ was expressed as % ID/g. To assess the presence of intact LanM protein, urine was directly injected to the radioHPLC. Eluate was collected in 30 s increments from 0–20 min. Activity in each tube was quantified using a γ-counter and the counts were used to reconstruct the metabolite trace, which was then compared to the original radiolabeled protein.

Table S2. Biodistribution of ^{132/135}La-LanM and ^{132/135}La-Citrate

Organ	^{132/135} La-LanM 2 h (n=3)	^{132/135} La-Citrate 2 h (n=3)
Blood	0.07 ± 0.03	0.32 ± 0.12
Heart	0.80 ± 0.13	2.15 ± 0.71
Lung	0.50 ± 0.19	1.57 ± 1.00
Liver	14.42 ± 3.60	38.67 ± 2.62
Spleen	0.48 ± 0.11	1.19 ± 0.39
Kidney	143.09 ± 4.49	15.95 ± 14.71
`Sm Int	0.38 ± 0.23	1.13 ± 0.50
Muscle	0.20 ± 0.04	0.46 ± 0.27
Bone	3.53 ± 0.49	9.07 ± 1.89

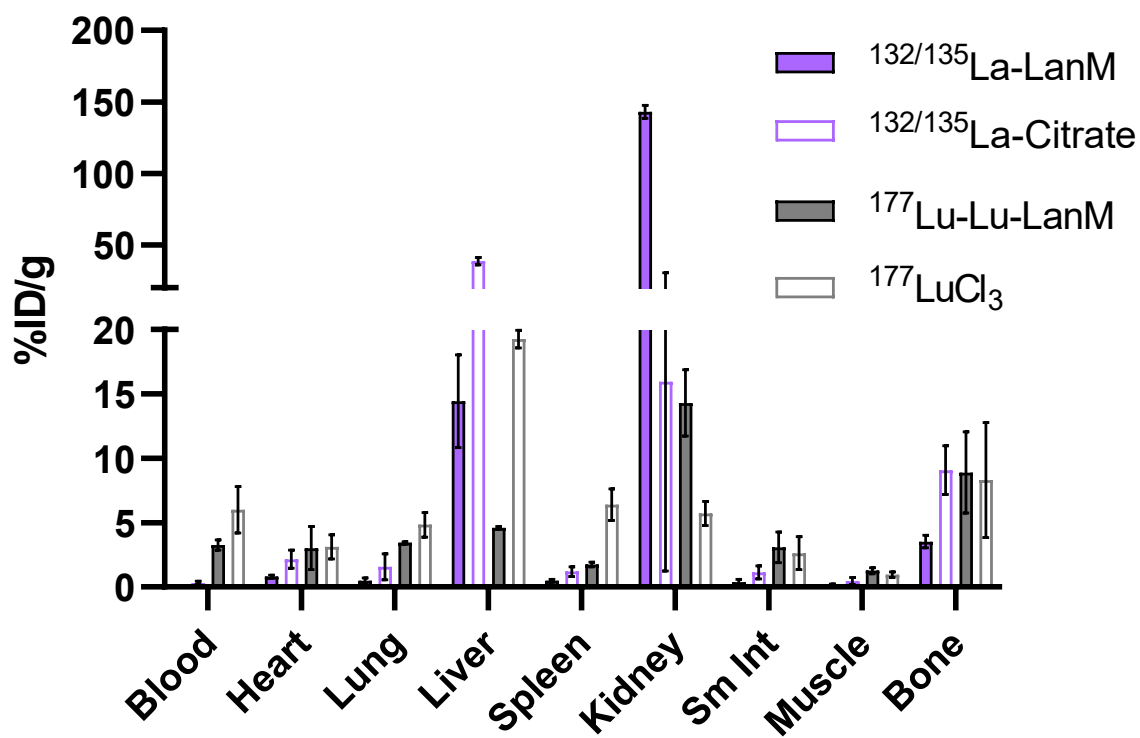


Figure S14. Comparative biodistribution of $^{132/135}\text{La-}$ and $^{177}\text{Lu-Lu-LanM}$.

8.3 $^{132/135}\text{La}$ Conjugate Targeted Biodistribution

Male mice (5 weeks old, Taconic, NCr nude male) were inoculated subcutaneously with PSMA+ PC3 PiP cells and PSMA- PC3 Flu cells (5.0×10^5 each) suspended in Matrigel and DPBS (1:2 DPBS: Matrigel), on the right and left shoulders, respectively. When tumors reached a suitable size, mice were injected with $^{132/135}\text{La}$ -LanM-PSMA (0.37-0.67 MBq/10-18 μCi) or $^{132/135}\text{La}$ -citrate (1.11-1.41 MBq/30-38 μCi). After 2 h, animals were sacrificed by cervical dislocation and selected tissues were collected and weighed. Activity of tissues was counted using a γ -counter (1470 PerkinElmer Wizard) and the radioactivity associated with each organ was expressed as % ID/g. To assess the presence of intact protein, urine was directly injected to the radioHPLC and eluate was collected in 30 s increments from 0–20 min. Activity in each tube was quantified using a γ -counter and the resulting reconstructed trace was compared to that of the radiolabeled protein.

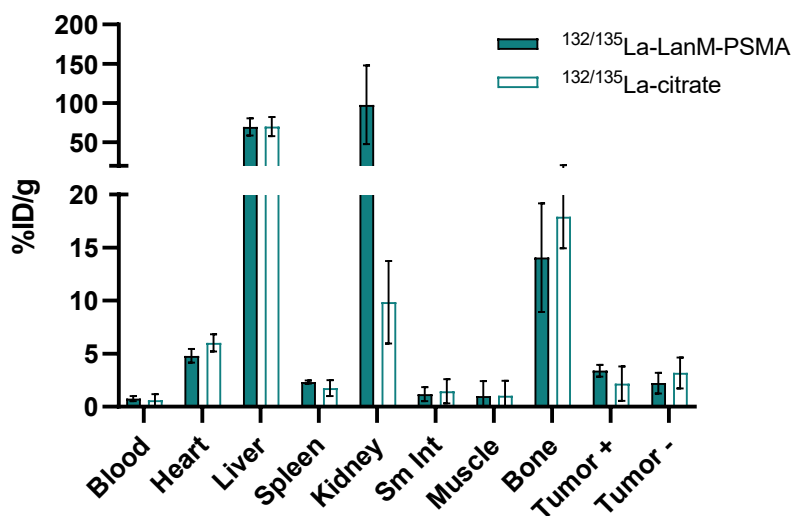


Figure S15. Biodistribution of $^{132/135}\text{La}$ -LanM-PSMA compared to $^{132/135}\text{La}$ -citrate.

Table S3. Biodistribution of $^{132/135}\text{La}$ -LanM-PSMA and $^{132/135}\text{La}$ -citrate

Organ	$^{132/135}\text{La}$ -LanM-PSMA 2 h (n=4)	$^{132/135}\text{La}$ -citrate 2 h (n=4)
Blood	0.76 ± 0.23	0.63 ± 0.55
Heart	4.80 ± 0.66	6.03 ± 0.81
Liver	69.59 ± 11.05	70.06 ± 12.22
Spleen	2.32 ± 0.15	1.75 ± 0.76
Kidney	97.74 ± 50.10	9.86 ± 3.89
Sm Int	1.18 ± 0.66	1.46 ± 1.13
Muscle	1.01 ± 1.39	1.05 ± 1.41
Bone	14.06 ± 5.13	17.93 ± 2.99
Tumor +	3.40 ± 0.55	2.18 ± 1.63
Tumor -	2.23 ± 0.98	3.19 ± 1.46

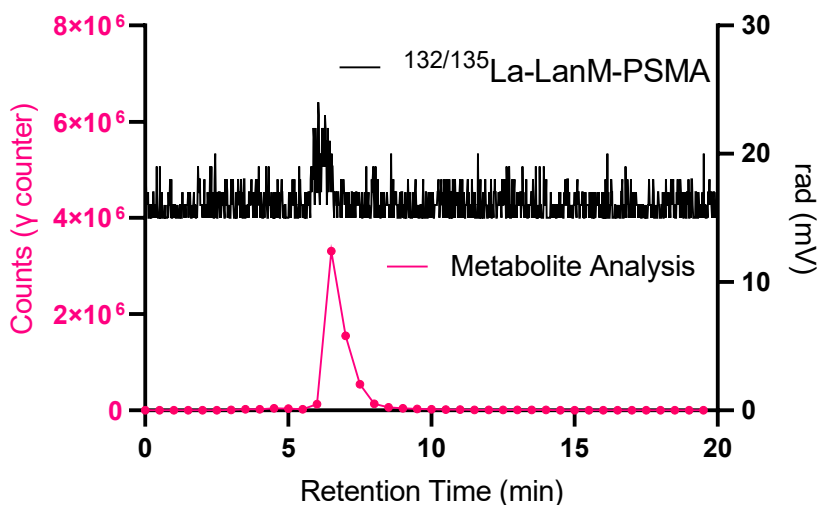


Figure S16. Metabolite analysis of $^{132/135}\text{La}$ -LanM-PSMA compared to radiolabeling trace.

8.4 ⁸⁹Zr Conjugate Naïve Biodistribution

Male mice (6 weeks old, Charles River, BALB/C) were injected with ⁸⁹Zr-DFO-LanM (0.9-1.5 MBq/25-40 μCi), or ⁸⁹Zr⁴⁺ (1.2-1.6 MBq/32-43 μCi). After 2 h, animals were sacrificed by cervical dislocation and selected tissues were collected and weighed. Activity of tissues was counted using a γ-counter (1470 PerkinElmer Wizard) and the radioactivity associated with each organ was expressed as % ID/g. To assess the presence of intact protein remaining, urine was directly injected to the radioHPLC and the resulting trace was compared to that of the radiolabeled protein.

Table S4. Biodistribution of ⁸⁹Zr-DFO-LanM and ⁸⁹Zr-oxalate

Organ	⁸⁹ Zr-DFO-LanM 2 h (n=5)	⁸⁹ Zr-oxalate 2 h (n=3)
Blood	0.32 ± 0.06	10.45 ± 1.06
Heart	0.52 ± 0.11	3.91 ± 0.86
Lung	0.52 ± 0.23	5.19 ± 1.58
Liver	0.68 ± 0.11	2.91 ± 0.52
Spleen	0.56 ± 0.16	1.46 ± 0.44
Kidney	84.15 ± 17.52	11.78 ± 7.45
Sm Int	0.42 ± 0.13	1.43 ± 0.20
Muscle	0.19 ± 0.14	2.03 ± 1.01
Bone	0.48 ± 0.07	6.23 ± 4.35

9. PET Imaging

Mice were imaged at 90 min post injection (p.i.) using Siemens Inveon PET/CT Multimodality System, and images were reconstructed using ASIPro software. Analysis of images were conducted using AMIDE.

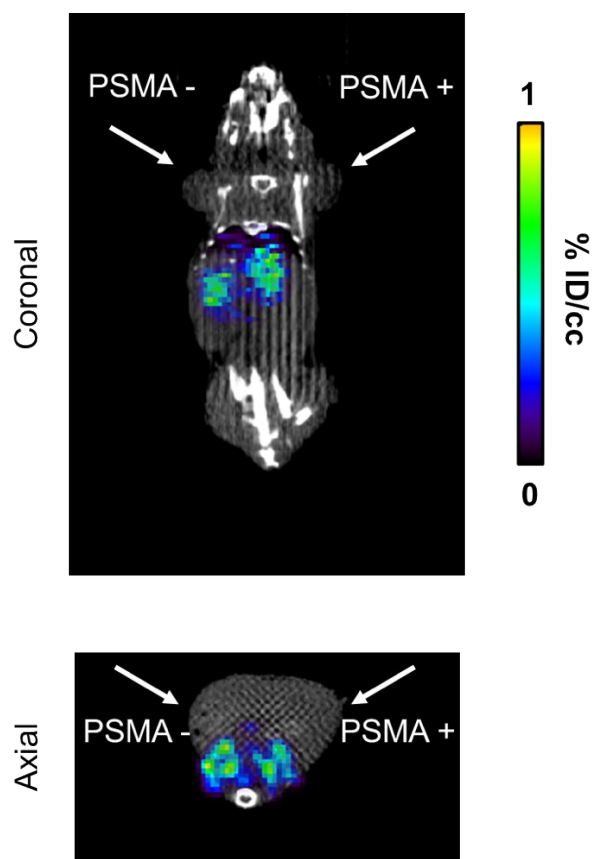


Figure S17. Single slice PET/CT images of $^{132/135}\text{La-LanM}$ in PC3 PIP (PSMA+, right) and PC3 Flu (PSMA-, left) subcutaneous tumor-bearing mice at 90 min p.i. Tumors are indicated by white arrows.

10. References

1. J. A. Cotruvo, E. R. Featherston, J. A. Mattocks, J. V. Ho and T. N. Laremore, *J. Am. Chem. Soc.*, 2018, **140**, 15056-15061.
2. Z. Dong, J. A. Mattocks, G. J.-P. Deblonde, D. Hu, Y. Jiao, J. A. Cotruvo and D. M. Park, *ACS Cent. Sci.*, 2021, **7**, 1798-1808.
3. E. R. Featherston, J. A. Mattocks, J. L. Tirsch and J. A. Cotruvo, in *Methods in Enzymology*, ed. J. A. Cotruvo, Academic Press, 2021, vol. 650, pp. 119-157.
4. D. Śmiłowicz, D. Schlyer, E. Boros and L. Meimetis, *Mol. Pharmaceutics*, 2022, **19**, 3217-3227.